Additive Manufacturing Letters 3 (2022) 100062

Contents lists available at ScienceDirect

Additive Manufacturing Letters

journal homepage: www.elsevier.com/locate/addlet

Multi-Process Printing Method Combining Powder and Resin Based Additive Manufacturing

John Whitehead*, Hod Lipson

Columbia University, 500 West 120th St, New York, NY 10027, USA

ARTICLE INFO

Keywords:
Selective laser sintering
SLS
Stereolithography
SLA
Multi-material
Resin
Powder

ABSTRACT

We propose a novel additive manufacturing (AM) method that combines both powder-based and resin-based printing processes. Both resin-based and powder-based processes have unique advantages ranging from strength and variety of materials for powder processes, to resolution and surface finish for resin printing. Previously, we proposed a novel powder-based printing process that directs a laser beam upwards to fuse powders through glass to a substrate. However, this setup can also be used to solidify resin as a secondary material in the same print. We demonstrate this hybrid process by fabricating samples containing both resins and powders. We also examine the potential for resin to be used to reduce powder bed fusion part porosity as well as adjust part surface finish. We discuss the impacts of these results and propose future uses.

1. Introduction

1.1. Printing Processes

The field of additive manufacturing (AM) comprises a wide range of processes and materials [1,2]. Two of the most versatile AM processes are laser-based powder bed fusion (here referred to as selective laser sintering or SLS) and resin printing (referred to as stereolithography or SLA). Both work by using a directed laser to construct parts layer by layer out of a fusible or curable substance until a solid object is formed [3,4]. However, each process requires different materials. SLA printing uses liquid resins that, once processed, solidify to generate rigid parts. SLS processes, on the other hand, produce parts that are comprised of fused material particles, and so can be made from a variety of meltable material families such as metallic alloys and some polymers [5,6].

Traditionally, users have been forced to select a single AM machine that uses a single printing process with a single type of material to produce a given part, and then add secondary materials to the printed object through post processing. This can be imprecise or time consuming depending on the adjustment method used.

Both processes have advantages and disadvantages. Selective laser sintering printers, for example, produce parts that have high strength and end-use potential when processing metallic and plastic powders, but suffer from poor surface finish and high porosity [7–10]. Stereolithography printers, on the other hand, generate parts with higher precision. This means that these parts beneficially have a smooth, solid surface finish. However, SLA prints are not necessarily as robust as printed SLS parts and are limited in the range of photocurable polymers [11–13]. Previous multi-material printer designs are similarly limited. While they may have access to a wider range of materials, these materials are generally in the same overall family (e.g. only resins, only powders, etc.) and therefore suffer from some flaw inherent to the base printing process (porosity, conductivity, etc.).

1.2. Multi-Process Printing

We have previously proposed a method that would allow multi-material SLS printing by inverting the print system [14,15]. Inverted Laser Sintering (ILS) allows us to sinter powdered material to a substrate from the top down, layer by layer, by fusing a thin layer of powder through a glass substrate. The hanging nature of the part and substrate also allows us to move the printed piece between material reservoirs, enabling multi-material printing capabilities. To accomplish this, material powder is first distributed on a glass sheet. A print substrate is lowered on top of the powder, compressing the powder between the substrate and the glass. A laser is directed up through the glass, sintering the material powder onto the substrate. The substrate is then raised with the sintered material and moved to a glass slide with a secondary material. The secondary material is exposed to either the same or a secondary laser, fusing it to either the substrate or the previously sintered material powder. This process can then be repeated until a solid part is generated.

Extending the ILS concept further, in this paper we present a process that allows us to print both SLA resins and SLS powders in the

* Corresponding author.
E-mail address: jdw2199@columbia.edu (J. Whitehead).

https://doi.org/10.1016/j.addlet.2022.100062
Received 8 April 2022; Received in revised form 25 May 2022; Accepted 26 May 2022
2772-3690/© 2022 The Authors. Published by Elsevier B.V. This is an open access article under the CC BY-NC-ND license (http://creativecommons.org/licenses/by-nc-nd/4.0/)

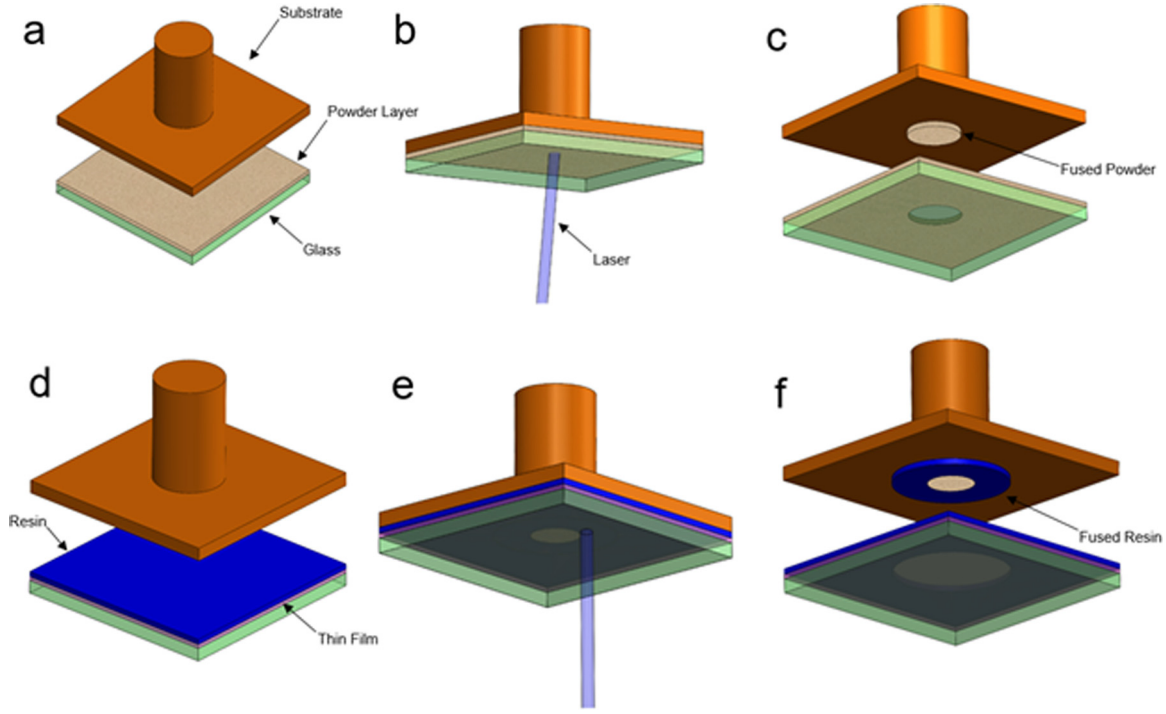


Fig. 1. Overview of the proposed multi-process AM. (a) Release agent coated glass and powder material layer captured by the release agent (b) Substrate is pressed onto the upper surface of the powder and the laser fuses a selected region of powder to the substrate (c) The substrate is raised with the fused powder (d) The substrate is moved to a separate slide which has a film on the upper surface which has been coated with resin (e) The substrate presses the sintered powder down into the resin and the laser is run again, towards the center of the glass it can be seen that the powder region has displaced some resin on the film (f) The resin can either be fused as a secondary layer on top of the powder or in the same layer around the powder. (For interpretation of the references to color in this figure, the reader is referred to the web version of this article).

same component. This is done by transporting a substrate between glass slides coated with resin and slides coated with powder, selectively fusing regions from each material onto the same print (Fig. 1). For clarity, in Fig. 1 we have colored the thin film purple and the glass green, however in reality these are both transparent. Utilizing SLA resins in addition to SLS powders allows for the printing of high-strength parts with smooth surface finishes, and widens the array of available materials that can be incorporated in a single object. This wider material array, in addition to surface finish, allows prints to possess a greater variety of properties, including varied conductivity throughout the part, variable strength and variable thermal resistivity. These properties can come from particulate materials, pure resins, or resins which have been adapted by the introduction of additional elements. Previous work in the area of combining these two processes involves first printing the SLS core component, and then transferring the part to a separate stereolithography machine which adds an outer, resin surface [16]. This process, however, inherently requires an external mechanism to transfer the part which can add cost or time, and limits the potential for printing SLA regions inside of the SLS parts. Furthermore, it is logistically challenging to print materials, especially fluidic ones, onto existing 3D components. Our process does not require this additional transport mechanism and its fully hybridized nature could allow for printing not only outer SLA regions but internal ones as well. We demonstrate this multi-material process by printing samples containing both powdered TPU (thermoplastic polyurethane) and resin. We also examine the possibility of using resin to reduce the porosity of SLS components.

2. Materials and Methods

Our testing setup requires a laser capable of transmitting through clear glass surfaces. We selected a blue 445 nm diode laser operating at ~1.2 amps, corresponding to ~1.3 W for the powder (J Tech Photonics). The same laser was used to process the resin, but the power output was reduced to 200 mW at ~0.2 amps. This laser selection was due to the fact that blue lasers have been shown to effectively process both thermoplastic powders and curable resins [17,18]. The beam's point was moved by a set of mirror galvanometers which were controlled using an Arduino UNO microcontroller. These mirrors were used to direct the beam upwards. The laser's operating state was controlled by a TTL input connected to the Arduino.

The glass selected was borosilicate glass, due to its low thermal conductivity [19]. We utilized 2″ x 2″ glass pieces with a 1/8″ thickness for all experiments. To prevent adhesion of the processed resin to the glass, a thin low density polyethylene film was placed between the uncured resin and the glass surface. This film allowed the cured resin to peel away from the glass without damage, similar to Formlabs' Low Force Stereolithography (LFS). To generate resin layers, a syringe was used to deposit 0.5 mL of liquid resin onto the middle of the film, with the resin then being allowed to distributed outward over the surface. Future iterations can include an automatic wiper blade or alternative method to ensure that the film is evenly coated. After processing, the film and the printed part/substrate were removed from the glass, and the film was peeled off of the print. This film could then be used in subsequent cycles after being cleaned with isopropyl alcohol. Occasionally, this film needed to be replaced due to wear.

For material powder deposition, a thin layer of aerosolized release agent (Water Soluble Mold Release Agent, SLIDE) was manually sprayed onto the glass, which was then coated with the selected material powder. This coating was accomplished by depositing an excess amount of powder onto the glass. A monolayer of this powder was fluidically captured by the release agent, and any excess material was disposed of. Substrates were initially fabricated from PLA plastic on a standard fused deposition modeling (FDM) printer.

Table 1
Processing parameters for the TPU and resin materials.

Material	φ (degrees)	Time (ms)	Scan Speed (deg/ms)	Nested Circle Distance (green to brown dots, mm)
TPU	1	5	0.2	0.31
Resin	5	1	5	0.31

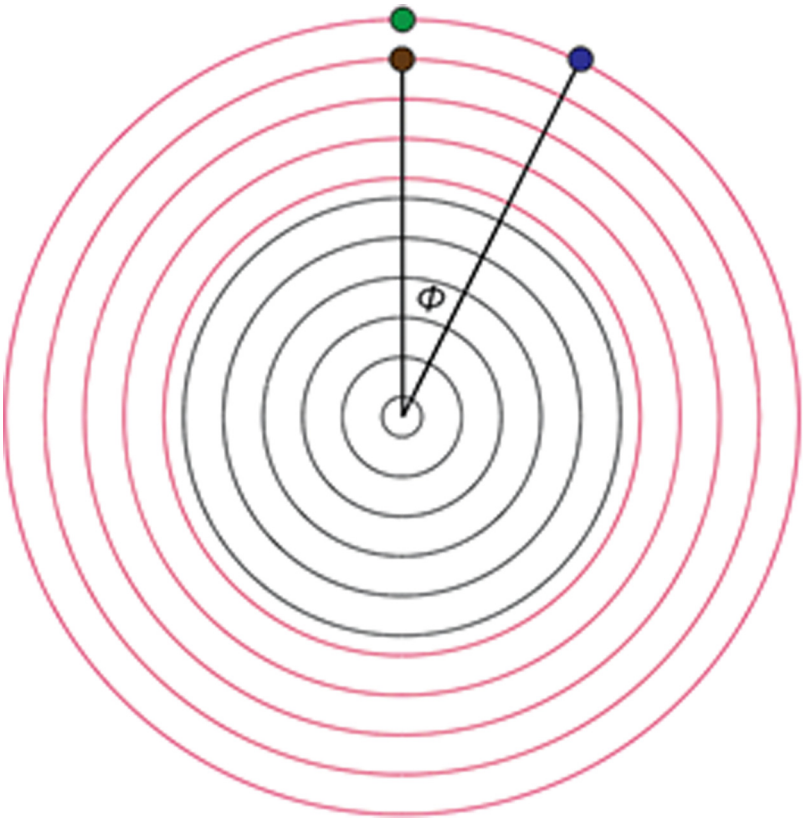


Fig. 2. Diagram of the laser processing pattern. The outer red rings denote the resin and the inner black rings represent the powder. The laser moves in a circle pattern in each layer before moving inwards towards the center. (For interpretation of the references to color in this figure, the reader is referred to the web version of this article).

To prove this concept, both resins and powders were needed. Initially, we selected white TPU powder (Sinterit) due to its relatively low melting point when compared to alternative materials such as metals, and its previous use in the ILS system [20]. For our resin, Formlabs draft resin was selected primarily due to its relatively high maximum layer thickness (~300 μm), which was necessary due to the manual nature of the material distribution and experimentation. The resin also has a contrasting color when compared to the TPU and is compatible with blue lasers.

During the printing process, the substrate was manually moved between the resin and powder glass plates. For this paper, we printed both these materials in a nested cylinder configuration. This geometry was selected to clearly display two distinct material regions in both external and profile images for better analysis. In this print, most layers consisted of an outer ring fabricated from resin and an inner ring comprised of fused powder. There was a single initial print layer fabricated from pure resin. The multi-material layer fabrication was accomplished by first placing the substrate (2″ x 2″) on the resin coated film/glass in the path of the laser and applying a fixed load (500 g) to the substrate to help further distribute the resin and ensure contact between the material and the substrate/previous layer. The laser was then run in a concentric/nested circle pattern to fuse the outer ring, and the print/substrate was lifted off the glass. The resin coated sheet of glass was then replaced by the powder/release agent coated glass. Excess resin was removed from the print/substrate, and the substrate and the fused material were placed down on the powder layer. A second load (1 kg) was applied to press the material against the substrate/previous layer. The laser was then directed up through the bottom of the glass into the powder layer, fusing the inner ring and completing the print layer.

Between concentric ring sintering cycles, excess, unfused material on the print/substrate was removed. For the excess resin, removal was accomplished by pressing the exposed print layers against an absorbent medium. For the powder, removal was done using a cotton applicator. Sintering was controlled by distance between successive circles (green to brown), and distance/time (as a function of φ) between sintering points (blue to green) in a given circle (Fig. 2). The laser parameters used for each of these materials is outlined in Table 1 and were determined experimentally. While keeping the scan speed constant would result in different exposure durations for the different nested circles, we concluded that we could still successfully process the material for the entire printing cycle at the given parameters. These parameters are relative to the center of the beam. Due to the fluid nature of the resin, some amount of "staining", where resin stains and permeates the fused powder is inevitable unless a post-curing or thorough cleaning apparatus is introduced into the process between cycles.

To better visualize resin penetration of powder layers, we fused a circular region of powder to a substrate and then printed a layer of resin on top of this powder. This was done using the same parameters as the nested cylinder print, with the draft resin and the TPU powder. These prints were sliced in half, leaving semicircular samples. The samples were then observed under a microscope to determine the effects of a coating layer of resin on fused powder. The substrates used here were fabricated from acrylic.

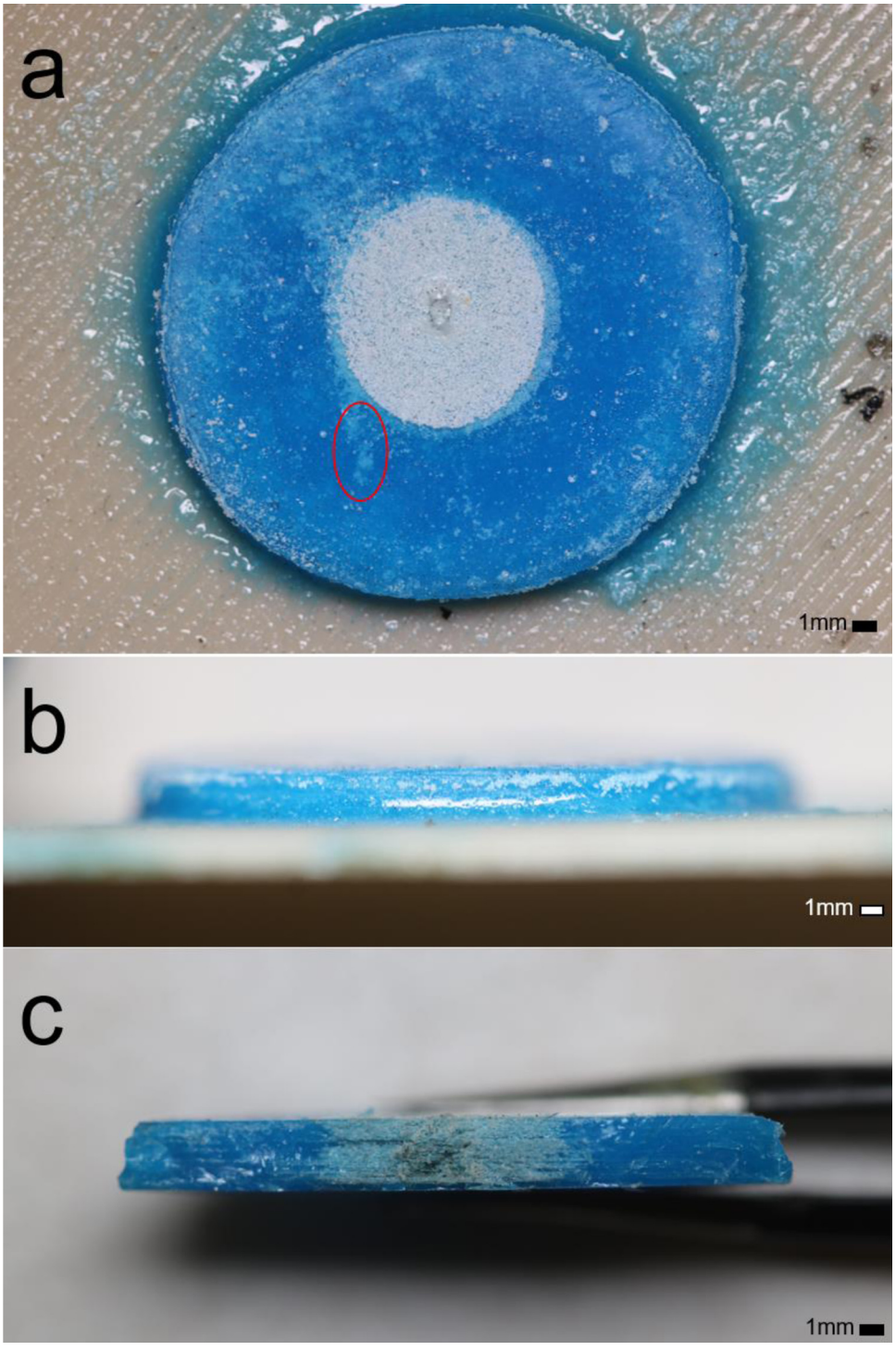


Fig. 3. Close up of result. (a) Upper view of the powder, resin nested cylinder. (b) Profile view of the nested cylinders (c) Sliced sample profile view. (For interpretation of the references to color in this figure, the reader is referred to the web version of this article).

3. Results

We printed a cylindrical print sample that had an inner cylindrical region composed of TPU powder and an outer region printed from SLA resin. This print had 30 layers, with an initial solid layer of resin included in this total. As the substrate was fabricated on an FDM printer, its outer surface was uneven and had several pores and voids. Therefore, this initial layer of resin was used to both create better adhesion to the substrate and to artificially fabricate a flat surface to build the rest of the print on. This is enabled by the conformal nature of the resin material. Due to the manual aspect of the print generation, the sample height deviated slightly from point to point. The average sample thickness was found to be ~2.86 mm which translated to an approximate average layer height of 95.3 μm. This thickness falls well within the resolution range for the draft resin. This height also is within the bounds for SLS layers, which typically range from 20 to 150 μm [21]. In order to better show the internal structure of the print sample, the print was cut in half (a cross sectional view is shown in Fig. 3c). It can be seen that in some regions the powder and resin layers overlap, likely due to factors including beam size and imperfect substrate placement. This resulted in sections where fused resin can be found between two layers of powder and vice versa. Additionally, due to the imprecise nature

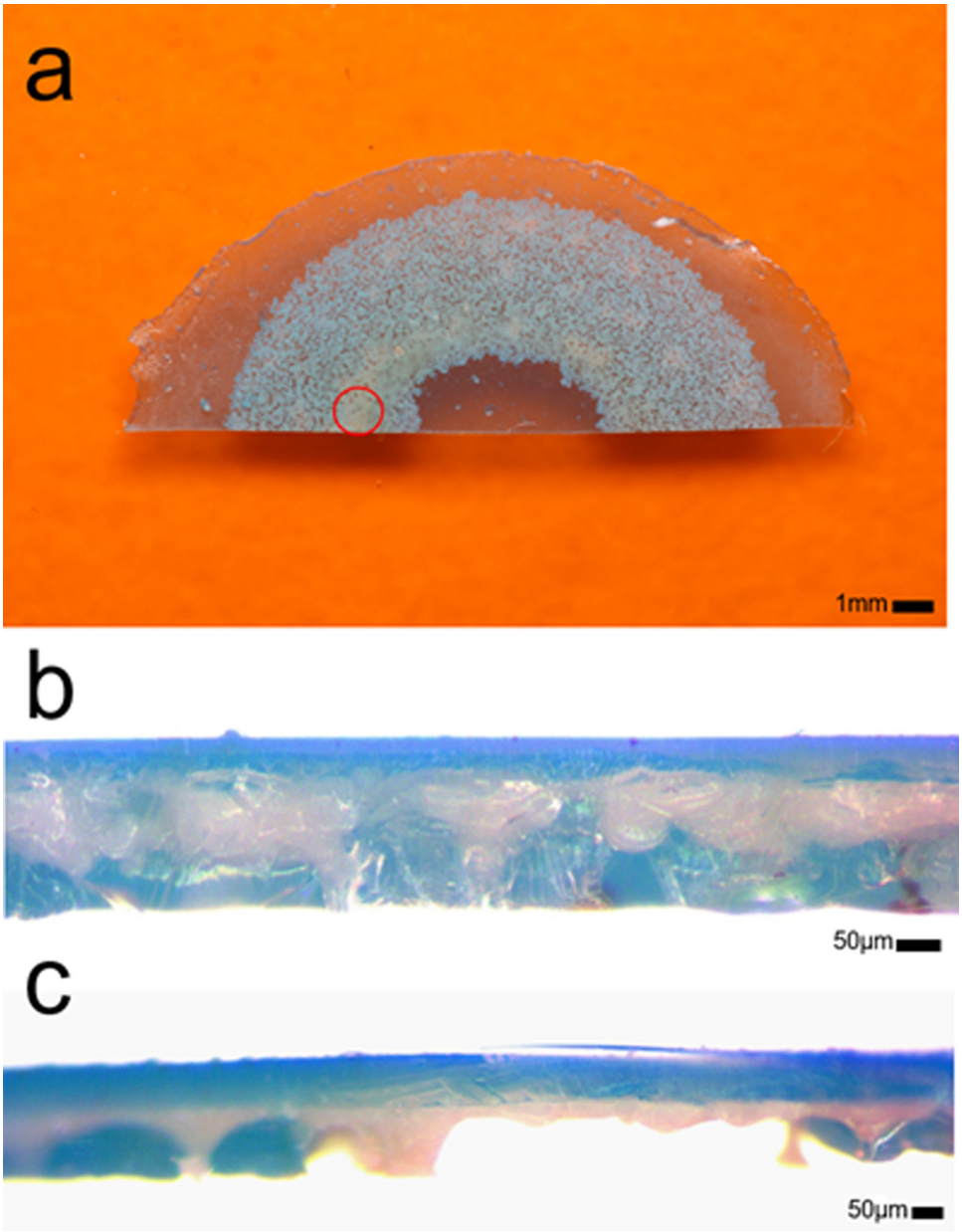


Fig. 4. Coating SLS parts using SLA. (a) Upper view of a resin-coated powder layer sample (b) Profile view of a sliced sample showing resin permeation (c) Print region without resin permeation.

of the testing setup, the outer ring (resin) and inner cylinder (powder) in a single layer might have moderately different heights, resulting in a difference that can compound to be significant over a larger number of layers. The slightly darkened regions towards the center of the TPU in both the top and sliced profile views is caused by overexposure of the material to the laser. This darkening/overexposure could be mitigated by varying parameters from nested circle to nested circle instead of keeping a constant scan speed. Doing so would ensure a more even exposure time throughout the sintering cycle. The layer boundaries also do not perfectly line up due to shifting of the substrate from layer to layer when it is manually placed back in the laser's path.

In addition to the nested print, we generated a series of samples that were comprised of an initial circular layer printed from TPU powder and a "sealing" layer printed from SLA resin (Fig. 4a). These samples were sliced in half and removed from the substrate. In order to observe their cross sections, they were viewed under an AmScope MU 1000 microscope. Close examination of a resin covered powder region highlights the staining effect, as it can be seen from the images that the resin has seeped into the fused powder, effectively filling some hollow, porous regions. The extent to which this filling occurs will depend heavily on the fused powder region's porosity and layer thickness. The resin also appears to have filled in under the powder layer at various points. Air bubbles trapped within the pores of the SLS layer prevent the resin from successfully permeating into the powder layer in some areas, as can be seen in the slightly lighter, discolored regions in the top view of the sliced sample (denoted by the red circle).

4. Discussion

One of the primary limitations of this process will be preventing or attempting to minimize cross-contamination. The fluidic nature of the resin, if not fully cured, can act in a similar fashion to the release agent, capturing stray particles. This can be seen in the white regions of the blue resin (one such region is circled in red, Fig. 3a). This powder can then become permanently trapped in the printed resin regions when the next layer of resin is added. Imperfect removal of resin can also cause thin, SLA layers between the SLS powder layers, which can be

seen in Fig. 3c. This could potentially affect layer to layer bonding of powder regions. It can also be seen that the layers are not perfectly aligned, which was likely caused by human error when placing the print/substrate on the new/unprocessed material layer. Additionally, staining can be seen in the profile view where the white core powder has been tinted. This is likely unavoidable without selective resin/powder deposition.

Due to the varied nature of the processes and materials, a potential problem for larger prints could be layer lag. Over time, without precise monitoring and correction, different regions fabricated from different materials in layer could have different thicknesses, which would contribute to print deformation and failure over a series of layers. This can additionally be caused by overlap, where one printed region overlaps with another, the layer thickness can be greater than the thickness of the rest of the layer. This can be a function of beam width and material distribution. This overlap, however, likely results in a higher bonding strength between the outer and inner cylinders, and so has potential value if compensated for. Use of the slicer program to generate samples instead of the fixed, cylindrical configuration can allow you to print more complex components.

When observing the single resin/powder layer sample, the fused powder can clearly be seen through the coating layer of resin. In order to obscure the TPU from view, several layers of resin or an alternative resin color choice would be required. The fact that the resin effectively permeated the powder in several areas, as well as filling in regions below the powder between the initial layer and the substrate has several practical implications. For one, the resin infusion gives the powder layer a smoother surface finish, and likely prevents fluid flow through the layer, making prints watertight and airtight. As can be seen in discolored regions, some areas had far less to no permeation, this could potentially be combatted by removing excess air in the print chamber through an ambient vacuum or intentional injection of material into the porous regions. However, the use of resin on the surface of the powder could affect powder layer bonding, and so the use of a resin layer on the outer edges of the print sample would likely be more advisable if surface finish was the primary concern.

Embedded powder in resin, additionally, could potentially have alternate uses if the powder is metal instead of a thermoplastic. Printing conductive channels made from metal into the resin (assuming a non-conductive resin) would allow for fully customizable, three-dimensional circuit boards. Furthermore, loosely sintering the powder channels or sintering the channels out of an easily dissolvable or otherwise removable materials could leave hollow channels or empty spaces in the resin printed part when the powder is removed. This would allow for embedded electronics or wire channels without the need for post assembly. The porous nature of the powder, as opposed to the resin, could also allow for some form of fluidic transport through the channels, with or without the removal of the powder material. Here, in effect, the powder would act primarily as a form of internal support structure.

5. Conclusion

We have successfully demonstrated that it is possible to print both SLA resins and SLS powders in the same test sample using an inverted laser setup. We have also demonstrated that doing so can directly influence porosity. This dramatically widens the available materials that can be incorporated into a single print. Greater material choice allows designers and engineers the freedom to choose exactly what properties they want in their print and where, including adjusting strength, surface finish and porosity. This has practical implications in several fields, including biomedical, aerospace and academia. While at the current juncture there is the issue of cross-contamination, future development of an automated setup should greatly reduce this issue. Also, incorporating metal powders instead of plastic would allow the user to print conductive channels directly inside of an insulating medium, resulting in items such as 3D printed circuit boards. Additionally, as there is a wide scope of possible resin formulations (i.e. ceramic resins, flexible print resins, water soluble resins, etc.) the properties that these multi-material prints can have is much wider than we demonstrate here.

Our next step will be to fully construct an inverted printer able to automatically generate components containing both powder and resins, this setup will have greater control over layer height, and will incorporate more robust cleaning methods to better prevent cross contamination.

Declaration of Competing Interest

The authors declare that they have no known competing financial interests or personal relationships that could have appeared to influence the work reported in this paper.

Acknowledgments

This work was supported in part by DARPA TRADES grant HR0011-17-2-0014, and DARPA MTO Lifelong Learning Machines Program W911NF-21-2-0071, as well as NSF NRI Award #1925157 and NSF AI Institute for Dynamical Systems #2112085.

References

[1] A. Busachi, J. Erkoyuncu, P. Colegrove, F. Martina, C. Watts, R. Drake, A review of additive manufacturing technology and cost estimation techniques for the defence sector, CIRP J. Manuf. Sci. Technol. 19 (2017) 117–128, doi:10.1016/j.cirpj.2017.07.001.
[2] M. Sireesha, J. Lee, A.S. Kiran, V.J. Babu, B.B. Kee, S. Ramakrishna, A review on additive manufacturing and its way into the oil and gas industry, RSC Adv. 8 (40) (2018) 22460–22468, doi:10.1039/c8ra03194k.
[3] T.D. Ngo, A. Kashani, G. Imbalzano, K.T. Nguyen, D. Hui, Additive manufacturing (3D printing): a review of materials, methods, applications and challenges, Compos. Part B Eng. 143 (2018) 172–196, doi:10.1016/j.compositesb.2018.02.012.
[4] N. Shahrubudin, T. Lee, R. Ramlan, An overview on 3D printing technology: technological, materials, and applications, Proced. Manuf. 35 (2019) 1286–1296, doi:10.1016/j.promfg.2019.06.089.
[5] F.P. Melchels, J. Feijen, D.W. Grijpma, A review on stereolithography and its applications in biomedical engineering, Biomaterials 31 (24) (2010) 6121–6130, doi:10.1016/j.biomaterials.2010.04.050.
[6] J. Kruth, X. Wang, T. Laoui, L. Froyen, Lasers and materials in selective laser sintering, Assem. Autom. 23 (4) (2003) 357–371, doi:10.1108/01445150310698652.
[7] G. Flodberg, H. Pettersson, L. Yang, Pore analysis and mechanical performance of selective laser sintered objects, Addit. Manuf. 24 (2018) 307–315, doi:10.1016/j.addma.2018.10.001.
[8] S. Eshraghi, S. Das, Mechanical and microstructural properties of polycaprolactone scaffolds with one-dimensional, two-dimensional, and three-dimensional orthogonally oriented porous architectures produced by selective laser sintering, Acta Biomater. 6 (7) (2010) 2467–2476, doi:10.1016/j.actbio.2010.02.002.
[9] J.H. Martin, B.D. Yahata, J.M. Hundley, J.A. Mayer, T.A. Schaedler, T.M. Pollock, 3D printing of high-strength aluminium alloys, Nature 549 (7672) (2017) 365–369, doi:10.1038/nature23894.
[10] W.E. Frazier, Metal additive manufacturing: a review, J. Mater. Eng. Perform. 23 (6) (2014) 1917–1928, doi:10.1007/s11665-014-0958-z.
[11] S. Zakeri, M. Vippola, E. Levänen, A comprehensive review of the photopolymerization of ceramic resins used in stereolithography, Addit. Manuf. 35 (2020) 101177, doi:10.1016/j.addma.2020.101177.
[12] J.C. Ruiz-Morales, A. Tarancón, J. Canales-Vázquez, J. Méndez-Ramos, L. Hernández-Afonso, P. Acosta-Mora, J.R. Marín Rueda, R. Fernández-González, Three dimensional printing of components and functional devices for energy and environmental applications, Energy Environ. Sci. 10 (4) (2017) 846–859, doi:10.1039/c6ee03526d.
[13] H. Wu, W. Liu, R. He, Z. Wu, Q. Jiang, X. Song, Y. Chen, L. Cheng, S. Wu, Fabrication of dense zirconia-toughened alumina ceramics through a stereolithography-based additive manufacturing, Ceram. Int. 43 (1) (2017) 968–972, doi:10.1016/j.ceramint.2016.10.027.
[14] J. Whitehead, H. Lipson, Inverted multi-material laser sintering, Addit. Manuf. 36 (2020) 101440, doi:10.1016/j.addma.2020.101440.
[15] amp J. Whitehead, H. Lipson, Embedding components during laser sintering, Addit. Manuf. Lett. (2022) 100055, doi:10.1016/j.addlet.2022.100055.
[16] M. Silva, R. Felismina, A. Mateus, P. Parreira, C. Malça, Application of a hybrid additive manufacturing methodology to produce a metal/polymer customized dental implant, Proced. Manuf. 12 (2017) 150–155, doi:10.1016/j.promfg.2017.08.019.
[17] N. Allahham, F. Fina, C. Marcuta, L. Kraschew, W. Mohr, S. Gaisford, A.W. Basit, A. Goyanes, Selective laser sintering 3D printing of orally disintegrating printlets containing ondansetron, Pharmaceutics 12 (2) (2020) 110, doi:10.3390/pharmaceutics12020110.

[18] T. Dostálová, M. Kasparova, K. Chleborad, M. Jelínek, P. Bradna, J. Mendricky, Intraoral scanner and stereographic 3D print in orthodontics, Lasers Dent. (2019) XXV, doi:10.1117/12.2507233.
[19] M.M. Smedskjaer, J.C. Mauro, R.E. Youngman, C.L. Hogue, M. Potuzak, Y. Yue, Topological principles of borosilicate glass chemistry, J. Phys. Chem. B 115 (44) (2011) 12930–12946, doi:10.1021/jp208796b.
[20] M. Schmid, A. Amado, K. Wegener, Polymer powders for Selective Laser Sintering (SLS), AIP Conference Proceedings (2015), doi:10.1063/1.4918516.
[21] S. Riza, S. Masood, C. Wen, Laser-assisted additive manufacturing for metallic biomedical scaffolds, Compr. Mater. Process. (2014) 285–301, doi:10.1016/b978-0-08-096532-1.01017-7.